Infectious Disease Modelling 7 (2022) 149–169

Contents lists available at ScienceDirect

Infectious Disease Modelling

journal homepage: www.keaipublishing.com/idm

Optimal control and cost-effective analysis of an age-structured emerging infectious disease model

Peiqi Jia [a, b], Junyuan Yang [a, b, *], Xuezhi Li [c]

[a] Complex Systems Research Center, Shanxi University, Taiyuan, 030006, Shanxi, PR China
[b] Shanxi Key Laboratory of Mathematical Techniques and Big Data Analysis on Disease Control and Prevention, Shanxi University, Taiyuan, 030006, PR China
[c] School of Mathematics and Information Science, Henan Normal University, Xinxiang, 453007, Henan, PR China

ARTICLE INFO

Article history:
Received 8 November 2021
Received in revised form 7 December 2021
Accepted 17 December 2021
Available online 25 December 2021
Handling editor: Dr Lou Yijun

Keywords:
Age-structured model
Admissible control
Ekerland variational principle
The basic reproduction number

ABSTRACT

Emerging infectious diseases are one of the global public health problems which may lead to widespread epidemics and potentially life-threatening infection. Integrated vaccination and physical distancing interventions are two elementary methods for preventing infectious diseases transmission. In this paper, we construct a continuous age-structured model for investigating the transmission dynamics of an emerging infection disease during a short period. We derive the basic regeneration number $\mathscr{R}_0$, the spectral radius of the next generation operator $\mathscr{K}$, which determines the disease outbreak or not. Furthermore, we propose an optimal control problem to take account for the cost-effectiveness of social distancing intervention and vaccination. We rigorously obtain sufficient conditions for a L^1 control problem. Numerical simulations show that coupling integrated vaccination and physical distancing intervention could effectively eliminate the infection, and such control strategy is more sensitive for people aged 10–39 and over 60.

1. Introduction

Emerging infectious diseases are infections that have recently appeared within a population or those whose incidence or geographic range is rapidly increasing or threatens to increase in the near future (Jones et al., 2008). Since 1940, there has been reported more than 335 emerging infectious diseases caused by pathogens, including newly evolved strains of pathogens (muti-strain resistent tuberculosis and chloroquine-resistent malaria), novel pathogens (HIV-1, SARS and COVID-19), and historically existing and recently increasing pathogens (Lyme and Ebola). The continuous outbreaks of emerging infectious diseases have led to some extremely serious impacts on global public health and economics. As reported, about 575,400 people worldwide died from H1N1 infection in 2009, SARS firstly reported in 2003 has spread more than 29 countries with 8096 cases and with 774 deaths, Ebola periodically appears and leads to more than 27,000 infectives and more than 11,000 deaths. Especially, COVID-19 has caused by a new coronavirus, and SARS-CoV-2 has resulted in more than 200 million cases and with 2.5 million deaths and it plausibly survives together with mankind. Hence, it is an ungent need to find

* Corresponding author. Complex Systems Research Center, Shanxi University, Taiyuan, 030006, Shanxi, PR China.
E-mail address: yjyang66@sxu.edu.cn (J. Yang).
Peer review under responsibility of KeAi Communications Co., Ltd.

https://doi.org/10.1016/j.idm.2021.12.004

suiTable quantitative and qualitative theories and approaches for exemplifying key principles and providing pertinent control measures.

The mathematical modeling of infectious diseases is an useful tool to understand the mechanisms of infectious diseases, which can anticipate their future development trend and evaluate control measures (Martcheva, 2015a). Pandemic H1N1 is transmitted by person-to-person (Fraser et al., 2009); Middle East Respiratory Syndrome-associated coronavirus (MERS-CoV) is driven by zoonotic infections from camels (Cauchemez et al., 2016); Ebola is spread through direct with serious sick or dead individuals (Agua-Agum et al., 2016); Zika virus has proved through mosquito-to-human (Majumder et al., 2018); COVID-19 can be transmitted by both person-to-person and environment-to-human (Eslami & Jalili, 2020). These identified mechanisms are in favor of understanding the principles of the disease dynamics and designing corresponding control strategies. To evaluate the seriousness of emerging infectious diseases, forecasting future epidemic trajectory and potential numbers of unobserved cases become an ungent issue. Bayesian probability models are usually employed to predict the incidence cases and correct the underestimations for fatality rate (Ghani et al., 2005). Facing an emerging infectious disease outbreak, one commonsense view is to develop a instant vaccine and exploit antiviral therapy, as well as improve the early detection, isolate the diagnosed cases and quarantine those individuals close contacting with confirmed cases for reducing the prevalence. Antimicrobial use and antiviral prophylaxis have been illustrated effectively to develop resistance and delay the spread of influenza pandemic (Glass et al., 2006) and it also involves social distancing measures such as isolation of suspected cases, school closures, travel restrictions and cancellation of mass gathering (Gojovic and SanderFisman, 2009). Massive vaccination has been extensively programmed to prevent the transmissions of COVID-19, HBV and HPV (Beutels, 1988; Lazarus et al., 2021).

Most of epidemic models have been assumed to be well-mixed with homogeneous disease infection between susceptibles and infectives. Generally, such homogeneous assumptions are suiTable to study the diseases well established in a population and it means that the transmission equally happens among humans, regardless of their age or any other behavior traits. However, some evidences and serological surveys have shown that the frequency of immunity to disease increases with age (Anderson & May 1974). The gradual increase of age-dependent variation in severity has been observed (Gao et al., 2016). The influenza mortality rate ranks children, young adults and the elderly (Oei & Nishiura, 2012). About 31–59% of the most severe symptomatic cases and particularly fatal cases of COVID-19 caused by SARS-Cov-2 have age from 75 to 84 (Ahmed et al., 2020). Understanding the role of age in transmission and disease severity is significant for determining the likely impact of social distancing interventions and vaccination programmes. Age-structured epidemic models have been proposed to characterize the heterogeneous transmission such as variable infectivity and variable susceptibility to infection (Li et al., 2020; Metz, 1978).

Response to an emerging infectious disease, policymakers and public health governments instantly take quarantine, isolation, treatment and vaccination for curbing the disease dispersion. Limitation to the knowledge of the disease, various resource production would likely be insufficient (Matrajt et al., 2021) and then effective disease controls will become a critical problem. The optimal control theory (Lev Semenovich Pontryagin, 1987; Wendell & Rishel, 2012) is a practical theory in epidemic control (Blayneh et al., 2009; Lenhart & Workman, 2007) with goals of reducing the deaths of infected individuals to project cost-effective intervention measures. Most of optimal control problems described by ordinary differential equations can be resolved by Pontryagins Maximum Principle, however, it is not always useful for studying such problems in L^1 space due to lack of the regularity of the solution of the state equations. As the aforementioned matter, age-heterogeneity is a key factor affecting the emerging infectious diseases spread. Hence, using time-dependent and age-specific control functions to measure the effectiveness of strategies is a feature of emerging infection disease model (Lee et al., 2012). Kwon et al. investigated the optimal treatment strategies with an age-structured model of HIV infection, and numerical simulations have demonstrated that the dynamic treatment strategy delays the peak arrival time of viral loads and reduces the sizes of that load (Kwon et al., 2012). Demasse et al. proposed three control strategies, such as minimizing immunization of young adults, the reduction of perinatal infection and treatment of HBV symptomatic infections, to optimize HBV-related deaths through the cost-effective analysis. They showed that mass vaccination in infants might be not enough to eradicate the virus, and an optimal control strategy is a combination of immunization of young adults and treatment of HBV symptomatic infections (Demasse et al., 2016).

The main contributions of this paper contain two aspects. One is that we construct a mathematical model to characterize the age-heterogeneity of an emerging infectious disease model and furthermore, we propose two age-time varying control measures-reducing social distance and mass vaccination to reduce the deaths of infected cases. To overcome the regularity problem of a L^1 control problem, we rigorously prove the existence of the optimal control and clarify the specific conditions of such existence by Ekerland variational principle.

The structure of this paper is organized as follows. In Section 2, we propose an age-structured model, calculate the basic reproduction number and completely study the global stability of the disease-free steady state. In Section 3, we take account for an optimal control problem dealing with mass vaccination efforts and reducing physical distancing. In this part, we take a great effort to prove the sufficient and necessary conditions of the existence of the optimal control pairs. Section 4 is conduct to the numerical experiments for identifying the optimal control strategies. The paper ends with a brief discussion in the last section.

2. Age-structured model formulation

In this paper, we focus on infections recently appeared within a population in a short period. In this case, we ignore the demography of the population, and consider the age heterogeneity.

Facing an emerging disease, vaccination is one of the effective control strategies for combating it. We divide the total population into six disjoint classes: susceptible, the latent, the infected, the hospitalized, the recovered and the vaccinated. $S(t, a)$ denotes the density of susceptibles of age a at time t; $E(t, a)$ denotes the density of the exposed of age a at time t; $I(t, a)$ denotes the density of infectives of age a at time t; $H(t, a)$ denotes the density of the hospitalized of age a at time t; $V(t, a)$ denotes the density of the vaccinated of age a at time t; $R(t, a)$ denotes the density of the recovered of age a at time t. Susceptibles with age a can be infected by infected individuals of age b at rate $\beta(a, b)$ and move to the exposed class. A susceptible is vaccinated at rate $\psi(a)$ and then becomes a vaccinator. The exposed transfer to the infected at rate $\alpha(a)$. Infectious individuals have been confirmed to be hospitalized individuals at rate $h(a)$, and both infected and hospitalized individuals are recovered at rate $\gamma(a)$ and die at rate $d(a)$. The vaccinated individuals can be infected at a reduced coefficient δ compared with an original infection. To address the above mechanisms, we propose an age-structured emerging disease model as follows:

$$\begin{cases} \dfrac{\partial S(t,a)}{\partial t} = -S(t,a)\displaystyle\int_0^{\omega} \beta(a,b)\frac{I(t,b)}{N(t,b)}db - \psi(a)S(t,a), \\ \dfrac{\partial E(t,a)}{\partial t} = (S(t,a)+\delta V(t,a))\displaystyle\int_0^{\omega} \beta(a,b)\frac{I(t,b)}{N(t,b)}db - \alpha(a)E(t,a), \\ \dfrac{\partial I(t,a)}{\partial t} = \alpha(a)E(t,a) - (h(a)+\gamma(a)+d(a))I(t,a), \\ \dfrac{\partial H(t,a)}{\partial t} = h(a)I(t,a) - (\gamma(a)+d(a))H(t,a), \\ \dfrac{\partial V(t,a)}{\partial t} = \psi(a)S(t,a) - \delta V(t,a)\displaystyle\int_0^{\omega} \beta(a,b)\frac{I(t,b)}{N(t,b)}db, \\ \dfrac{\partial R(t,a)}{\partial t} = \gamma(a)H(t,a) + \gamma(a)I(t,a), \end{cases} \tag{2.1}$$

where ω is the maximal active age for a person. System (2.1) has the following initial and boundary conditions:

$$S(0,a) = S_0(a), \quad E(0,a) = E_0(a), \quad I(0,a) = I_0(a),$$
$$H(0,a) = H_0(a), \quad V(0,a) = V_0(a), \quad R(0,a) = R_0(a).$$

The total population $N(t, a) = S(t, a) + E(t, a) + I(t, a) + H(t, a) + V(t, a) + R(t, a)$ satisfies

$$\frac{\partial N(t,a)}{\partial t} + \frac{\partial N(t,a)}{\partial a} = -d(a)[I(t,a)+H(t,a)],\ N(0,a) = N_0(a).$$

To study the dynamics of model (2.1), we make following assumptions on the model parameters from biological and mathematical view of points.

Assumption 2.1. (1) The functions $\beta \in C_{BU}(\mathbb{R}_+ \times \mathbb{R}_+, \mathbb{R}_+)$, where C_{BU} is the set of all bounded and uniformly continuous functions from $\mathbb{R}_+ \times \mathbb{R}_+$ to $\mathbb{R}_+$(2) $\psi(\cdot), \alpha(\cdot), h(\cdot), d(\cdot), \gamma(\cdot) \in L^{\infty}_{+}(\mathbb{R}_+)$, $L^{\infty}_{+}(\mathbb{R}_+)$ is the positive cone of $L^{\infty}(\mathbb{R}_+)$.

Obviously, system (2.1) always has the following disease-free equilibrium E_0:

(1) If $\psi(a) = 0$, system (2.1) has a disease-free equilibrium $E^{01} = (S^0(a), 0, 0, 0, 0, 0)$;
(2) If $\psi(a) \neq 0$, system (2.1) has a disease-free equilibrium $E^{02} = (0, 0, 0, 0, V^0(a), 0)$.

Linearising system (2.1) around E^{01} in the disease invasion phase, we have that

$$\begin{cases} \dfrac{\partial E(t,a)}{\partial t} = S^0(a)\displaystyle\int_0^{\omega} \beta(a,b)\frac{I(t,b)}{N_0(b)}db - \alpha(a)E(t,a), \\ \dfrac{\partial I(t,a)}{\partial t} = \alpha(a)E(t,a) - (h(a)+\gamma(a)+d(a))I(t,a), \end{cases} \tag{2.2}$$

where $N_0^{(a)}$ is the initial total population with age a. Let us define a linear operator $F : \mathbb{R}_+ \to \mathbb{R}_+$ by

$$F[\varphi](a) = S^0(a)\int_0^{\omega} \beta(a,b)\frac{\varphi(b)}{N_0(b)}db.$$

Dropping off the term F and solving the first equation of (2.2) result in

$$E(t,a) = E_0(a)e^{-\alpha(a)t}. \tag{2.3}$$

Substituting (2.3) into the second equation of (2.2), we obtain

$$I(t,a) = I_0(a)e^{-(h(a)+\gamma(a)+d(a))t} + E_0(a)\left(1-e^{-\alpha(a)t}\right). \tag{2.4}$$

Without loss of generation, let us assume $E_0(a) = 0$ for any $a \in \mathbb{R}_+$. Hence, the inverse of V is calculated by

$$V^{-1}[I](a) = \int_0^{\infty} I(t,a)dt = \frac{I_0(a)}{h(a)+\gamma(a)+d(a)}.$$

Therefore, the next generation operator $\mathscr{K}$ is defined by

$$\mathscr{K}[\varphi](a) = FV^{-1}[\varphi](a) = S_0(a)\int_0^{\omega} \frac{\beta(a,b)\varphi(b)}{N_0(b)(h(b)+\gamma(b)+d(b))}db. \tag{2.5}$$

Thus, the reproduction number $\mathscr{R}_{01}$ is defined by

$$\mathscr{R}_{01} = \rho(\mathscr{K}), \tag{2.6}$$

where ρ denotes the spectral radius. Similarly, let us proceed the above process around the other disease-free equilibrium E^{02}. We obtain the reproduction number for Case (2) as follows

$$\mathscr{R}_{02} = \rho(\mathscr{K}_1), \tag{2.7}$$

where

$$\mathscr{K}_1[\varphi](a) = \delta V_0(a)\int_0^{\omega} \frac{\beta(a,b)\varphi(b)}{N_0(b)(h(b)+\gamma(b)+d(b))}db.$$

Theorem 2.1. *Let $\mathscr{R}_{0j}(j=1,2)$ be defined in equations* (2.6) *and* (2.7). *If $\mathscr{R}_{0j}<1(j=1,2)$, then the disease-free equilibrium $E^{0j}(j=1,2)$ is locally asymptotically stable.*

Proof. Linearising system (2.1) around E^{01}, one reaches

$$\begin{cases} \dfrac{\partial s(t,a)}{\partial t} = -S_0(a)\displaystyle\int_0^{\omega}\beta(a,b)\frac{i(t,b)}{N_0(b)}db, \\ \dfrac{\partial e(t,a)}{\partial t} = S_0(a)\displaystyle\int_0^{\omega}\beta(a,b)\frac{i(t,b)}{N_0(b)}db - \alpha(a)e(t,a), \\ \dfrac{\partial i(t,a)}{\partial t} = \alpha(a)e(t,a) - (h(a)+\gamma(a)+d(a))i(t,a), \\ \dfrac{\partial h(t,a)}{\partial t} = h(a)i(t,a) - (\gamma(a)+d)h(t,a). \end{cases} \tag{2.8}$$

Letting $s(t,a) = x(a)e^{\lambda t}$, $e(t,a) = y(a)e^{\lambda t}$, $i(t,a) = z(a)e^{\lambda t}$, and $h(t,a) = l(a)e^{\lambda t}$, and then replacing them in (2.8), one arrives at

$$\begin{cases} \lambda x(a) = -S_0(a)\displaystyle\int_0^{\omega}\frac{\beta(a,b)z(b)}{N_0(b)}db, \\ (\lambda+\alpha(a))y(a) = S_0(a)\displaystyle\int_0^{\omega}\beta(a,b)\frac{z(b)}{N_0(b)}db, \\ (\lambda+(h(a)+\gamma(a)+d(a))z(a) = \alpha(a)y(a), \\ (\lambda+(\gamma(a)+d(a))l(a) = h(a)z(a). \end{cases} \tag{2.9}$$

If $\lambda \neq -(h(a)+\gamma+d(a))$, one has that

$$z(a) = \frac{\alpha(a)y(a)}{\lambda+h(a)+\gamma(a)+d(a)}.$$

Replacing z(a) in the second equation of (2.9) leads to

$$(\lambda+\alpha(a))y(a) = S_0(a)\int_0^{\omega}\beta(a,b)\frac{\alpha(b)y(b)}{(\lambda+h(b)+\gamma+d(b))N_0(b)}db := \mathscr{K}[\alpha y](a). \tag{2.10}$$

Suppose by argument, provided (2.10) has an eigenvalue λ with non-negative real parts, then the left modulus of (2.10) is larger than $\|\alpha(\cdot)y(\cdot)\|_{L^1}$. On the other hand, the right side of (2.10) is less $\|\alpha(\cdot)y(\cdot)\|_{L^1}$ if $\mathscr{R}_0 < 1$. This leads to a contradiction. Hence, the roots of equation (2.10) have only negative real parts.

If $\lambda = -(h(a)+\gamma(a)+d(a))$, then one has that $y(a) = 0$ for a.e. $a \in \mathbb{R}_+$. From the second and the fourth equations of (2.9), it follows that

$$z(a) = l(a) = 0, a.e. a \in \mathbb{R}_+.$$

Substituting these quantities into the first equation of (2.9), one must concludes that $x(a) = 0$, for a.e. $a \in \mathbb{R}_+$, or $\lambda = 0$. The first case is impossible since $(x,y,z,l)^T$ is an eigenvector associated an eigenvalue λ. For the last case, for $\varepsilon > 0$ small enough, then for any $\int_0^{\omega}|s_0(a)-x(a)|da < \varepsilon/2$,

$$\int_0^{\omega}|s(t,a)-x(a)|da \le \int_0^{\omega}|s(t,a)-s_0(a)| + |s_0(a)-x(a)|da = 2\int_0^{\omega}|s_0(a)-x(a)|da < \varepsilon. \tag{2.11}$$

Therefore, for any case, the disease-free equilibrium E^{01} is locally asymptotically sTable if $\mathscr{R}_{01} < 1$.

Proceeding the similar process, we can conclude the local stability of E^{02} if $\mathscr{R}_{02} < 1$. This completes the Proof.

Theorem 2.2. *Suppose $d(a) = 0$ for all $a \in \mathbb{R}_+$. If $\mathscr{R}_{0j} < 1 (j = 1, 2)$, then the disease-free equilibria E^{0j} is globally asymptotically stable.*

Proof. Provided $\psi(a) = 0$ for any $a \in \mathbb{R}_+$, then we have from the first and fifth equations known that for $a \in \mathbb{R}_+$,

$$S(t,a) \le S^0(a), \lim_{t\to+\infty} V(t,a) = 0.$$

If d(a) = 0, adding all the equations of (2.1) yields to $\partial N_t(t, a) = 0$, and so that $N(t, a) = N_0(a)$ for each pair $(t,a)\in\mathbb{R}^2_+$. From Assumption 2.1, we have known that $\mathscr{K}_1$ has a positive left eigenvector Ω(a) associated with $\mathscr{R}_{01}$ such that

$$\Omega(a)\mathscr{K}[\varphi](a) = \mathscr{R}_{01}\varphi(a)\Omega(a).$$

Now, we construct a Lyapunov functional as follows

$$L[E,I] = \int_0^\omega \Omega(a)[E(t,a)+I(t,a)]da.$$

Taking the derivative of L along the trajectory of (2.1), one arrives at

$$\begin{aligned}\frac{\partial L[E,I]}{\partial t}|_{(2.1)} &= \int_0^\omega \Omega(a)\left[\frac{\partial E(t,a)}{\partial t}+\frac{\partial I(t,a)}{\partial t}\right]da\\ &\le \int_0^\omega \Omega(a)(\mathscr{K}[(\gamma(a)+h(a))I](t,a) - (\gamma(a)+h(a))I(t,a))da + \varepsilon\omega \qquad (2.12)\\ &= \int_0^\omega \Omega(a)(\mathscr{R}_{01}-1)(\gamma(a)+h(a))I(t,a)da + \varepsilon\omega.\end{aligned}$$

From the arbitrary of ε, we have that $\partial L_t \le 0$ and the equality holds if and only if I(t, a) = 0 for $(t,a)\in\mathbb{R}^2_+$. Therefore, the largest invariant set $\mathscr{M} = \{\varphi\in X \,|\, \dot{L} = 0\}$ contains a singleton point E^{01}. By LaSalle invariant principle, we have that the disease-free equilibrium E^{01} is globally attractive when $\mathscr{R}_{01} < 1$ and d(a) = 0.

Similarly, we conclude that the disease-free equilibrium E^{02} is also globally asymptotically sTable if $\mathscr{R}_{02} < 1$.

3. An optimal control problem

3.1. Model with interventions

As mentioned in Introduction, we introduce such two strategies: reducing physical distance and taking mass vaccination to find an optimal intervention through minimizing the disease-related deaths and the costs for control implementation. Then, an age-structured epidemic model with two kinds of intervention strategies is described by the following system:

$$\begin{cases}\dfrac{\partial S(t,a)}{\partial t} = -S(t,a)\displaystyle\int_0^\omega \beta(a,b)(1-u_1(t,b))\frac{I(t,b)}{N(t,b)}db - (1+u_2(t,a))\psi(a)S(t,a),\\ \dfrac{\partial E(t,a)}{\partial t} = (S(t,a)+\delta V(t,a))\displaystyle\int_0^\omega \beta(a,b)(1-u_1(t,b))\frac{I(t,b)}{N(t,b)}db - \alpha(a)E(t,a),\\ \dfrac{\partial I(t,a)}{\partial t} = \alpha(a)E(t,a) - (h(a)+\gamma(a)+d(a))I(t,a),\\ \dfrac{\partial H(t,a)}{\partial t} = h(a)I(t,a) - (\gamma(a)+d(a))H(t,a),\\ \dfrac{\partial V(t,a)}{\partial t} = (1+u_2(t,a))\psi(a)S(t,a) - \delta V(t,a)\displaystyle\int_0^\omega \beta(a,b)(1-u_1(t,b))\frac{I(t,b)}{N(t,b)}db,\\ \dfrac{\partial R(t,a)}{\partial t} = \gamma(a)H(t,a) + \gamma(a)I(t,a),\end{cases} \qquad (3.1)$$

where u_1 and u_2 denote the two control variables of age a and time t. The parameters and state variables remain the same meaning as model (2.1).

Setting x(t, •) = (S(t,•); E(t,•); I(t,•); H(t,•); V(t,•); R(t,•))^T, system (3.1) becomes

$$\begin{cases} \partial_t x(t,a) = f(t,a,x(t,a),u_1(t,a),u_2(t,a)) := f(t,a), \\ x(t,0) = 0, \\ x(0,\cdot) = x^0(\cdot) := (S(0,\cdot); E(0,\cdot); I(0,\cdot); H(0,\cdot); V(0,\cdot)), \end{cases} \tag{3.2}$$

where

$$f(t,a) := \begin{pmatrix} -S(t,a)\int_0^\omega \beta(a,b)(1-u_1(t,b))\frac{I(t,b)}{N(t,b)}db - (1+u_2(t,a))\psi(a)S(t,a) \\ (S(t,a)+\delta V(t,a))\int_0^\omega \beta(a,b)(1-u_1(t,b))\frac{I(t,b)}{N(t,b)}db - \alpha(a)E(t,a) \\ \alpha(a)E(t,a) - (h(a)+\gamma(a)+d(a))I(t,a) \\ h(a)I(t,a) - (\gamma(a)+d(a))H(t,a) \\ (1+u_2(t,a))\psi(a)S(t,a) - \delta V(t,a)\int_0^\omega \beta(a,b)(1-u_1(t,b))\frac{I(t,b)}{N(t,b)}db \\ \gamma(a)H(t,a) + \gamma(a)I(t,a) \end{pmatrix}.$$

3.2. An optimal control question

As stated above, our goal is to find an optimal control strategy corresponding to age a and time t that minimizes both the deaths due to disease and the costs of epidemic controls. We apply L[1] optimal control theory to determine the "best" vaccination regime and physical distancing interventions. To achieve this goal, we define the objective function by such two interventions as follows:

$$J[u_1(t,a),u_2(t,a)] = \int_0^{T_f}\int_0^\omega M(t,a,x,u_1,u_2)dadt, \tag{3.3}$$

with

$$M(t,a,x,u_1,u_2) = B[d(a)I(t,a)+d(a)H(t,a)] + \frac{A_1}{2}u_1^2(t,a) + \frac{A_2}{2}u_2^2(t,a) + A_3\psi(a)S(t,a),$$

where B, A_1, A_2, A_3 are balancing coefficients and T_f counts the final time. The first sum in the integral is the cost of disease-related deaths and the last three terms represent costs of vaccination and physical distancing interventions.

To derive the necessary optimality condition, we introduce a time-varying and age-varying Lagrange multiplier vector $\zeta(t,a) = (\lambda_S(t,a),\lambda_E(t,a),\lambda_I(t,a),\lambda_H(t,a),\lambda_V(t,a),\lambda_R(t,a))^T$, whose elements are called the adjoint variables of system (3.1). Next, we define a generalized Hamiltonian function as follows:

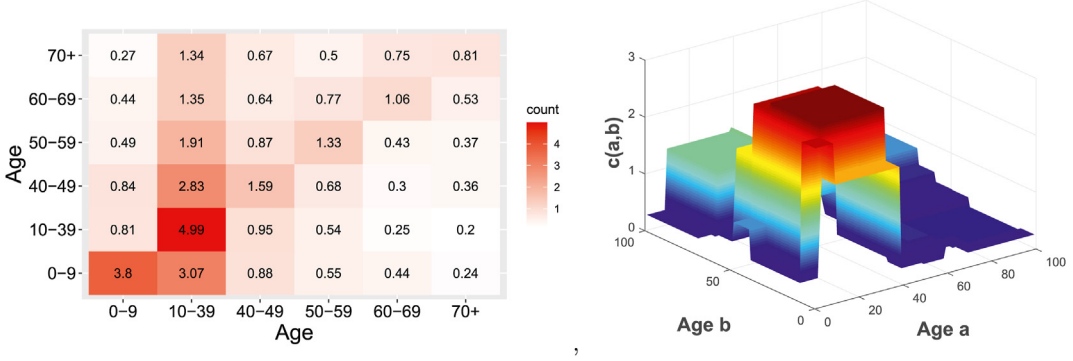

Fig. 1. The contact matrix among six different age groups.

Table 1
Definitions and values of parameters.

Symbols	Parameters	Values	Unites	Sources
β	infection rate	0.086 9	day^{-1}	Rocha Filho et al. (2020)
d	disease deduced death rate	0.017	day^{-1}	Epidemiology Team. The ep (2020)
ψ	vaccination rate	0.03	day^{-1}	Rocha Filho et al. (2020)
δ	rate of loss of immunity	1/180	day^{-1}	Rocha Filho et al. (2020)
1/α	latent period	5	day^{-1}	Linton et al. (2020)
1/h	diagnostic period	3.3	day^{-1}	Linton et al. (2020)
1/γ	recovery period	17.5	day^{-1}	Wang et al. (2020)

Table 2
Initial values of state variables.

Parameter	Value	Parameter	Value	Parameter	Value
$S_1(0)$	2983 907	$S_2(0)$	11 009 702	$S_3(0)$	2965 179
$E_1(0)$	1780	$E_2(0)$	1495	$E_3(0)$	1170
$I_1(0)$	356	$I_2(0)$	299	$I_3(0)$	234
$H_1(0)$	0	$H_2(0)$	3	$H_3(0)$	5
$V_1(0)$	89 517	$V_2(0)$	330 291	$V_3(0)$	88 955
$R_1(0)$	0	$R_2(0)$	2	$R_3(0)$	4
$S_4(0)$	2243 257	$S_5(0)$	1285 473	$S_6(0)$	998 712
$E_4(0)$	890	$E_5(0)$	755	$E_6(0)$	750
$I_4(0)$	178	$I_5(0)$	151	$I_6(0)$	150
$H_4(0)$	11	$H_5(0)$	21	$H_6(0)$	39
$V_4(0)$	67 297	$V_5(0)$	38 564	$V_6(0)$	29 961
$R_4(0)$	9	$R_5(0)$	17	$R_6(0)$	32

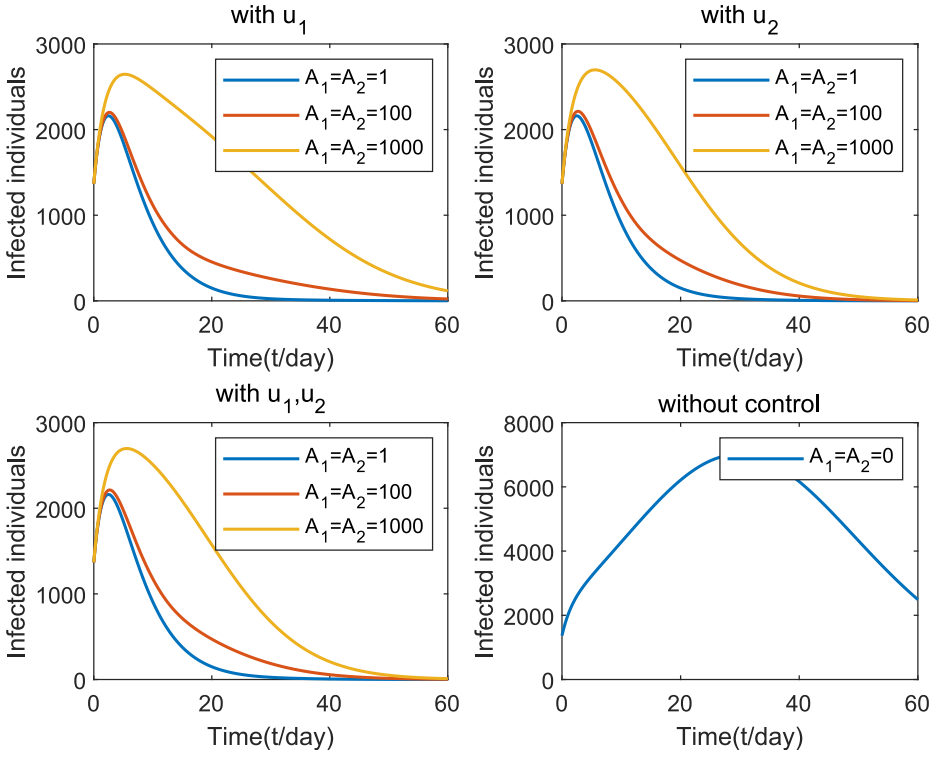

Fig. 2. Curves of the total number of infections with different weights under strategy A-D with control parameter in three cases: (1) Low cost: $A_1 = A_2 = 1$; (2) Moderate cost: $A_1 = A_2 = 100$; (3) High cost: $A_1 = A_2 = 1000$. The weight parameters are fixed as $A_3 = B = 1$.

Table 3
Objective function values with different costs under strategy A-D.

Objective function	Low cost	Moderate cost	High cost
Strategy A	17 930 120	17 930 300	17 931 852
Strategy B	10 855 028	10 856 863	10 862 809
Strategy C	10 853 586	10 853 714	10 862 018
Strategy D	17 997 930	17 997 930	17 997 930

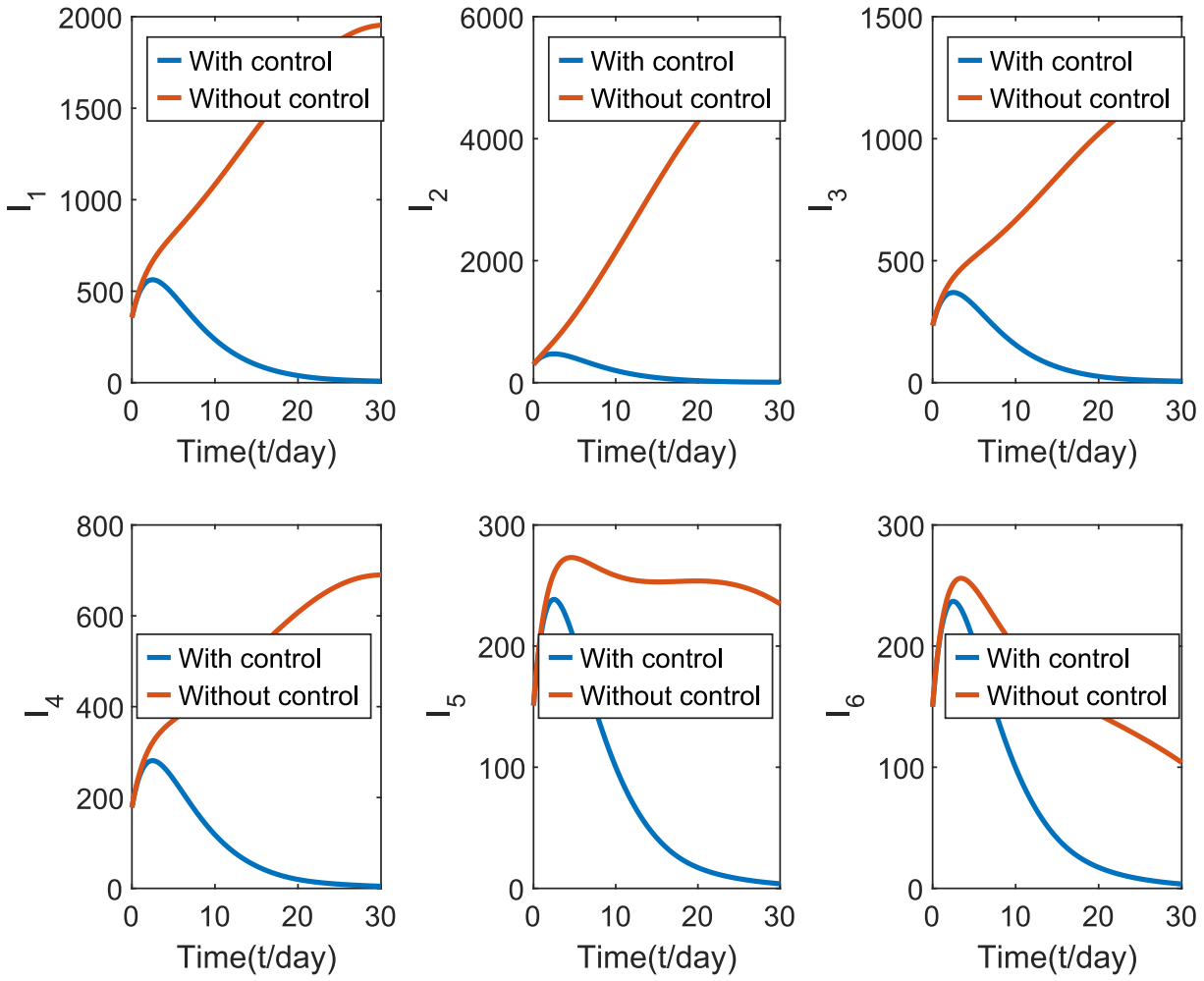

Fig. 3. Epidemic curves of infected individuals in different age groups under strategy C. The red solid curves represent the infected number $I_j(t)$, j = 1, 2, …, 6 without control, the blue lines denote the infectives $I_j(t)$, j = 1, 2, …, 6, with strategy C. The parameters are fixed at $A_1 = A_2 = A_3 = B = 1$.

$$
\begin{aligned}
&\mathscr{H}(t,a) = M(t,a,x,u_1,u_2) + \zeta(t,a)\cdot f(t,a)\\
&= B(d(a)I(t,a) + d(a)H(t,a)) + \frac{A_1}{2}u_1^2(t,a) + \frac{A_2}{2}u_2^2(t,a) + A_3\psi(a)S(t,a)\\
&+\lambda_S(t,a)\left(-S(t,a)\int_0^{\omega}\beta(a,b)(1-u_1(t,b))\frac{I(t,b)}{N(t,b)}db - (1+u_2(t,a))\psi(a)S(t,a)\right)\\
&+\lambda_E(t,a)\left((S(t,a)+\delta V(t,a))\int_0^{\omega}\beta(a,b)(1-u_1(t,b))\frac{I(t,b)}{N(t,b)}db - \alpha(a)E(t,a)\right)\\
&+\lambda_I(t,a)(\alpha(a)E(t,a) - (h(a)+\gamma(a)+d(a))I(t,a))\\
&+\lambda_H(t,a)(h(a)I(t,a) - (\gamma(a)+d(a))H(t,a))\\
&+\lambda_V(t,a)\left((1+u_2(t,a))\psi(a)S(t,a) - \delta V(t,a)\int_0^{\omega}\beta(a,b)(1-u_1(t,b))\frac{I(t,b)}{N(t,b)}db\right)\\
&+\lambda_R(t,a)(\gamma(a)H(t,a) + \gamma(a)I(t,a)),
\end{aligned}
\tag{3.4}
$$

where $\cdot$ represents an inner product. Let $\triangle_x$ denotes the differentiation with respect to variable x. The adjoint system is given by

$$
\begin{cases}
-\partial_t\zeta(t,a) = \triangle_x M(t,a) + \zeta(t,a)\cdot\triangle_x f(t,a),\\
\zeta\left(T_f,a\right) = 0, \zeta(t,\omega) = 0,
\end{cases}
\tag{3.5}
$$

that is

Table 4
Biomass under strategy C.

Age group	The total number of infection	The number of people who avoid becoming infected	IAR
0–9	5644	40 201	0.860
10–39	4739	93 559	0.949
40–49	3715	24 793	0.850
50–59	2830	15 388	0.816
60–69	2404	75 664	0.968
≥ 70	2389	52 010	0.954

Table 5
Correlation values under different strategies.

Strategy	The total number of infection	The number of people who avoid becoming infected	Objective function
Strategy A	21 858	379 679	17 930 120
Strategy B	87 149	314 388	10 855 028
Strategy C	21 844	379 693	10 853 586
Strategy D	401 537	–	17 997 930

$$
\begin{aligned}
-\frac{\partial\lambda_S(t,a)}{\partial t} = & \Big(\int_0^{\omega}\beta(a,b)(1-u_1(t,b))\frac{I(t,b)}{N(t,b)}db - S(t,a)\int_0^{\omega}\beta(a,b)(1-u_1(t,b))\\
& \times\frac{I(t,b)}{N^2(t,b)}db\Big)(\lambda_E(t,a)-\lambda_S(t,a))+\psi(a)(1+u_2(t,a))(\lambda_V(t,a)-\lambda_S(t,a))+A_3\psi(a)\\
& +\delta V(t,a)\int_0^{\omega}\beta(t,b)(1-u_1(t,b))\frac{I(t,b)}{N^2(t,b)}db(\lambda_V(t,a)-\lambda_E(t,a)),\\
-\frac{\partial\lambda_E(t,a)}{\partial t} = & S(t,a)\int_0^{\omega}\beta(a,b)(1-u_1(t,b))\frac{I(t,b)}{N^2(t,b)}db(\lambda_S(t,a)-\lambda_E(t,a))+\alpha(a)(\lambda_I(t,a)-\lambda_E(t,a))\\
& +\delta V(t,a)\int_0^{\omega}\beta(a,b)(1-u_1(t,b))\frac{I(t,b)}{N^2(t,b)}db(\lambda_V(t,a)-\lambda_E(t,a)),\\
-\frac{\partial\lambda_I(t,a)}{\partial t} = & Bd(a)+S(t,a)\int_0^{\omega}\beta(a,b)(1-u_1(t,b))\Big(\frac{1}{N(t,b)}db(\lambda_E(t,a)-\lambda_S(t,a))-\frac{I(t,b)}{N^2(t,b)}\Big)db\\
& +\delta V(t,a)\int_0^{\omega}\beta(a,b)(1-u_1(t,b))\Big(\frac{1}{N(t,b)}db-\frac{I(t,b)}{N^2(t,b)}\Big)db(\lambda_E(t,a)-\lambda_V(t,a))\\
& -(h(a)+\gamma(a)+d(a))\lambda_I(t,a)+\gamma(a)\lambda_R(t,a)+h(a)\lambda_H(t,a),\\
-\frac{\partial\lambda_H(t,a)}{\partial t} = & Bd(a)+S(t,a)\int_0^{\omega}\beta(a,b)(1-u_1(t,b))\frac{I(t,b)}{N^2(t,b)}db(\lambda_S(t,a)-\lambda_E(t,a))\\
& +\delta V(t,a)\int_0^{\omega}\beta(a,b)(1-u_1(t,b))\frac{I(t,b)}{N^2(t,b)}db(\lambda_V(t,a)-\lambda_E(t,a))\\
& -(\gamma(a)+d(a))\lambda_H(t,a)+\gamma(a)\lambda_R(t,a),\\
-\frac{\partial\lambda_V(t,a)}{\partial t} = & S(t,a)\int_0^{\omega}\beta(a,b)(1-u_1(t,b))\frac{I(t,b)}{N^2(t,b)}db(\lambda_S(t,a)-\lambda_E(t,a))\\
& +\delta\Big(\int_0^{\omega}\beta(a,b)(1-u_1(t,b))\frac{I(t,b)}{N(t,b)}db\\
& -V(t,a)\int_0^{\omega}\beta(a,b)(1-u_1(t,b))\frac{I(t,b)}{N^2(t,b)}db\Big)(\lambda_E(t,a)-\lambda_V(t,a)),\\
-\frac{\partial\lambda_R(t,a)}{\partial t} = & S(t,a)\int_0^{\omega}\beta(a,b)(1-u_1(t,a))\frac{I(t,b)}{N^2(t,b)}db(\lambda_S(t,a)-\lambda_E(t,a))\\
& +\delta V(t,a)\int_0^{\omega}\beta(a,b)(1-u_1(t,a))\frac{I(t,b)}{N^2(t,b)}db(\lambda_V(t,a)-\lambda_E(t,a))
\end{aligned}
$$

with the following transversality conditions and boundary conditions:

$$
\begin{cases}
\lambda_S\big(T_f,a\big) = & \lambda_E\big(T_f,a\big)=\lambda_I\big(T_f,a\big)=\lambda_H\big(T_f,a\big)=\lambda_V\big(T_f,a\big)=0,\\
\lambda_S(t,\omega) = & \lambda_E(t,\omega)=\lambda_I(t,\omega)=\lambda_H(t,\omega)=\lambda_V(t,\omega)=0.
\end{cases}
\tag{3.6}
$$

Then, the optimal control pairs satisfy $\frac{\partial\mathscr{H}}{\partial u_1}=0$ and $\frac{\partial\mathscr{H}}{\partial u_2}=0$, which read in forms of

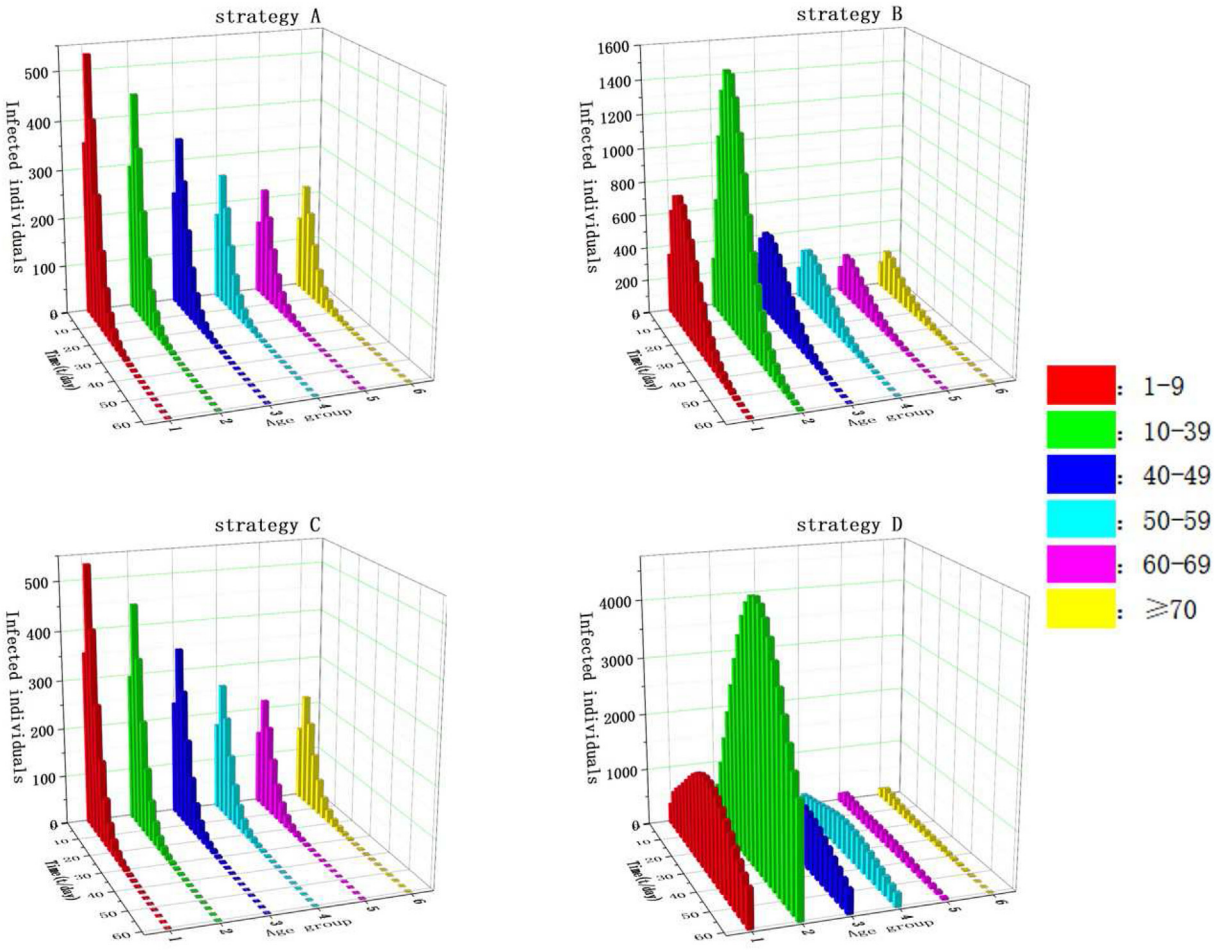

Fig. 4. The 3-d prism of the number of infected individuals in different age groups under strategy A-D. The parameters are fixed at $A_1 = A_3 = B = 1$, $A_2 = 1000$.

$$\hat{u}_1(t,a) = \frac{((\lambda_E(t,a) - \lambda_S(t,a))S(t,a) + (\lambda_E(t,a) - \lambda_V(t,a))\delta V(t,a)) \int_0^{\omega} \beta(t,b)\frac{I(t,b)}{N(t,b)}db}{A_1}, \tag{3.7}$$

$$\hat{u}_2(t,a) = \frac{\psi(a)S(t,a)(\lambda_S(t,a) - \lambda_V(t,a))}{A_2}. \tag{3.8}$$

From the set of the admissible control, the optimal control pair is characterized by the following formula:

$$u_1^* = \min\{\max\{0, \hat{u}_1\}, 1\},$$

$$u_2^* = \min\{\max\{0, \hat{u}_2\}, 1\}.$$

3.3. The sufficient conditions for the optimal control

In this subsection, we search for control pairs (u_1^*, u_2^*) definitely satisfying

$$J(u_1^*, u_2^*) = \min_{/\!/} J(u_1, u_2), \tag{3.9}$$

on the control set

Table 6
The durations of strong controls in different age groups.

Control	0 – 9 years old	10 – 39 years old	40 – 49 years old
physical distance	24.24	27.24	22.14
vaccination	51.66	57.18	51.66
Control	50 – 59 years old	60 – 69 years old	over 70 years old
physical distance	20.64	18.48	17.16
vaccination	49.62	45.12	42.78

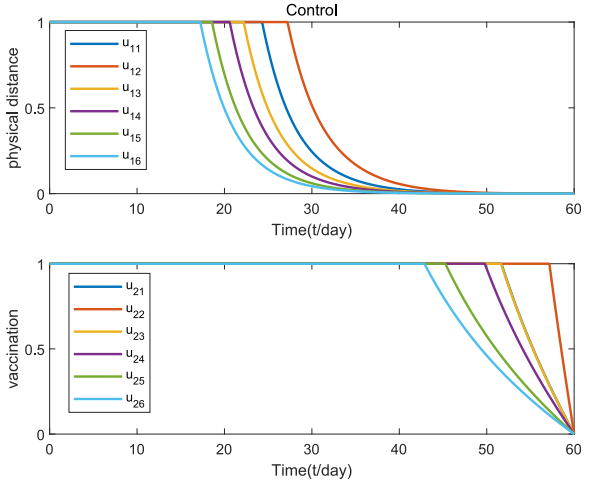

Fig. 5. The curves of control variables of different age groups under optimal control strategy C.

$$\mathscr{U} = \{(u_1, u_2 \in L^\infty(Q)) : 0 \le u_1(\cdot, a) \le u_{1max}(a) \le 1; 0 \le u_2(\cdot, a) \le u_{2max}(a) \le 1\},$$

where $Q = [0, T_f] \times [0, \omega]$, $u_{jmax}(\cdot)$, $j = 1, 2$ are given measurable positive functions.

Setting a control vector by $u := (u_1, u_2) \in \mathscr{U}$, and corresponding state variables and adjoint variables are denoted by x^u and λ^u respectively, we define

$$\mathscr{L} : L^1(Q) \times L^1(Q) \longrightarrow$$

by $\mathscr{L}(U_1, U_2) = (\mathscr{L}_1 U_1, \mathscr{L}_2 U_2)$ with

$$\mathscr{L}_i U_i = \begin{cases} 0, & \text{if } U_i < 0, \\ U_i, & \text{if } 0 \le U_i \le u_{imax}, i = 1, 2 \\ u_{imax}, & \text{if } U_i \ge u_{imax}, \end{cases}$$

and $Q = [0, T_f] \times [0, \omega]$.

We define the norm $\| \cdot \|_{L^1(\mathscr{X})}$ for $\mathscr{X} := Q^5$ as follow:

$$\| x \|_{L^1(\mathscr{X})} = \int_Q \sum_{i=1}^5 |x_i(t, a)| da dt,$$
$$\| x \|_{L^\infty(\mathscr{X})} = \sum_{i=1}^5 \sup_{(t,a) \in Q} |x_i(t, a)|,$$

for each $x := (x_1, \ldots, x_5) \in \mathscr{X}$. Accordingly, we can define the norms $\| \cdot \|_{L^1(\mathscr{U})}$, $\| \cdot \|_{L^\infty(\mathscr{U})}$ similarly.

Then, we embed the optimal problem in space $L^1(Q)$ by

$$\mathscr{J}(U)=\begin{cases} J(u), & \text{if } u\in\mathscr{U},\\ +\infty, & \text{if } u\notin\mathscr{U}.\end{cases}$$

Before proving the existence of the optimal control, we introduce the following lemma.

Lemma 1. *Setting T_f be sufficiently small, the following statements are true.*

(1) *The map $u\in\mathscr{U}\to x^u\in L^1(\mathscr{X})$ satisfies Lipschitz properties:*

$$\| x^u - x^v\|_{L^1(\mathscr{X})} \le C_x^1 \| u - v\|_{L^1(\mathscr{U})},$$

$$\| x^u - x^v\|_{L^\infty(\mathscr{X})} \le C_x^\infty \| u - v\|_{L^\infty(\mathscr{U})},$$

for all $u,v\in\mathscr{U}$.

(2) *For $u\in\mathscr{U}$, adjoint system has a weak solution λ^u in $L^\infty(\mathscr{X})$, such that*

$$\| \lambda^u - \lambda^v\|_{L^\infty(\mathscr{X})} \le C_\lambda^\infty \| u - v\|_{L^\infty(\mathscr{U})},$$

for all $u,v\in\mathscr{U}$.

(3) *The functional $\mathscr{J}(u)$ is lower semi-continuous with respect to $L^1(\mathscr{L})$ convergence.*

Proof. Letting $x^j=(S^j,E^j,I^j,H^j,V^j)\in L^1(\mathscr{X})$, and

$$\Gamma^j(a,t)=\int_0^\omega \beta(a,b)(1-j(t,b))\frac{I^j(t,b)}{N^j(t,b)}db \le \bar{\beta}\omega := M_\Gamma^j, j=u,v. \tag{3.10}$$

We have that

$$\begin{aligned}
\|\Gamma^u(a,t)-\Gamma^v(a,t)\|_{L^\infty(\mathscr{X})} &= \sup_{t\in[0,T_f],a\in[0,\omega]}\int_0^\omega \beta(a,b)\left[(1-u_1(t,b))\frac{I^u(t,b)}{N^u(t,b)}-(1-v_1(t,b))\frac{I^v(t,b)}{N^v(t,b)}\right]db\\
&\le \sup_{t\in[0,T_f],a\in[0,\omega]}\int_0^\omega \beta(a,b)\left\{2\frac{I^u(t,b)}{N^u(t,b)}-\frac{I^v(t,b)}{N^v(t,b)}+\left|u_1(t,a)-v_1(t,a)\right|\right\}db\\
&\le \sup_{t\in[0,T_f],a\in[0,\omega]}2\int_0^\omega \beta(a,b)\left\{\frac{I^u(t,b)-I^v(t,b)}{N^u(t,b)}+\frac{I^v(t,b)N^u(t,b)-N^v(t,b)}{N^v(t,b)N^u(t,b)}\right\}db\\
&\quad +\|u_1(t,a)-v_1(t,a)\|_{L^\infty(\mathscr{U})}\\
&\le \bar{\beta}|\Omega|\left(4\underline{N}\|N^u(t,b)-N^v(t,b)\|_{L^\infty(Q)}+\left\|u_1(t,a)-v_1(t,a)\right\|_{L^\infty(\mathscr{U})}\right)\\
&\le C_\Gamma^\infty\left(\left\|x^u(t,a)-x^v(t,a)\right\|_{L^\infty(\mathscr{X})}+\left\|u_1(t,a)-v_1(t,a)\right\|_{L^\infty(\mathscr{U})}\right).
\end{aligned}$$

Do the similar process, we have known that

$$\|\Gamma^u(a,t)-\Gamma^v(a,t)\|_{L^1(\mathscr{X})}\le C_\Gamma^1\left(\left\|x^u(t,a)-x^v(t,a)\right\|_{L^1(\mathscr{X})}+\left\|u_1(t,a)-v_1(t,a)\right\|_{L^1(\mathscr{U})}\right).$$

From the first equation of (3.1), we integrate from 0 to t and obtain

$$S^j(t,a) = S_0(a) - \int_0^t S^j(x,a)\Gamma^j(a,x)dx - \psi(a)\int_0^t (1+j(x,a))S^j(x,a)dx, j = u, v.$$

Hence, we have that

$$\begin{aligned}
&\|S^u(t,a) - S^v(t,a)\|_{L^\infty(Q)} \\
&= \sup_{t\in[0,T_f],a\in[0,\omega]} |S^u(x,a)\Gamma^u(a,x) - S^v(x,a)\Gamma^v(a,x)|dx + \sup_{t\in[0,T_f],a\in[0,\omega]} \psi(a)\int_0^t |(1+u_2(x,a))S^u(x,a) - (1+v_2(x,a))S^v(x,a)|dx \\
&\le \sup_{t\in[0,T_f],a\in[0,\omega]} (M_\Gamma^u + \psi)T_f|S^u(t,a) - S^v(t,a)| + \sup_{t\in[0,T_f],a\in[0,\omega]} \bar{N}T_f|\Gamma^u(a,t) - \Gamma^v(a,t)| + \sup_{t\in[0,T_f],a\in[0,\omega]} \bar{N}T_f|u_2(t,a) - v_2(t,a)| \\
&\le C_S^\infty\left(\left\|x^u(t,a) - x^v(t,a)\right\|_{L^\infty(\mathscr{X})} + \left\|u_2(t,a) - v_2(t,a)\right\|_{L^\infty(\mathscr{U})}\right).
\end{aligned}$$

Proceeding the analogous process, we have that

$$\|L^u - L^v\|_{L^\infty(Q)} \le C_L^\infty\left(\left\|x^u(t,a) - x^v(t,a)\right\|_{L^\infty(\mathscr{X})} + \left\|u(t,a) - v(t,a)\right\|_{L^\infty(\mathscr{U})}\right), L = E, I, H, V.$$

Collecting all the mentioned above, one arrives at

$$\|x^u(t,a) - x^v(t,a)\|_{L^\infty(\mathscr{X})} \le C_x^\infty\|u(t,a) - v(t,a)\|_{L^\infty(\mathscr{U})}.$$

Replacing L^∞ norm by L^1 norm, we repeat the above programs to get

$$\|x^u(t,a) - x^v(t,a)\|_{L^1(\mathscr{X})} \le C_x^1\|u(t,a) - v(t,a)\|_{L^1(\mathscr{U})}.$$

For Case (2), we observe that

$$\frac{\partial N(t,a)}{\partial t} = -d(a)(I(t,a) + H(t,a)) \ge -d(a)N(t,a),$$

which suggests that $N_0(a)e^{-d(a)t} \le N(t, a) \le N_0(a)$ for all $(t,a)\in\mathbb{R}_+^2$.

$$\left\|\frac{\partial L(t,a)}{\partial t}\right\| \le C_L, L = S, E, I, H, V, \tag{3.11}$$

$$\left\|\frac{\partial \lambda_L(t,a)}{\partial t}\right\| \le C_Z, Z = \lambda^S, \lambda^E, \lambda^I, \lambda^H, \lambda^V, \tag{3.12}$$

Observing that for any $0 < u_j < u_{jmax}$, $j = 1, 2$, one can easily derive the following equation

$$\frac{\partial \lambda_L}{\partial t} = \frac{\partial \lambda_L}{\partial u_j}\frac{\partial u_j}{\partial t}.$$

For the convenience, let us denote

$$\frac{\partial \lambda_L}{\partial u_j} = f_{Lu_j}, L = S, E, I, H, V, j = 1, 2.$$

From formulas (3.7) and (3.8), it follows that $\|f_{Lu_j}\|_{L^\infty(Q)} \le \hat{C}_{Lu_j}, L = S,E,I,H,V, j = 1,2$. If $u_j \le 0$ or $u_j \ge u_{jmax}$, j = 1, 2, we have from continuous dependence of solutions λ_L(L = S, E, I, H, V) on parameters u_j(j = 1, 2) that $\|f_{Lu_j}\|_{L^\infty(Q)} \le \tilde{C}_{Lu_j}, L = S,E,I,H,V, j = 1, 2$.

From what has been discussed, one concludes that for every u,

$$\|f_{Lu_j}\|_{L^\infty(Q)} \le C_{Lu_j},$$

where $C_{Lu_j} = \max\{C_{Lu_j}, \tilde{C}_{Lu_j}\}$, L = S, E, I, H, V, j = 1, 2. Therefore, for any $(t,a) \in \mathbb{R}^2_+$,

$$\|\lambda^u(t,a) - \lambda^v(t,a)\|_{L^\infty(\mathscr{X})} \le C^\infty_\lambda \|u(t,a) - v(t,a)\|_{L^\infty(\mathscr{U})},$$

where $C^\infty_\lambda := \max_{L=S,E,I,H,V, j=1,2}\{C_{Lu_j}\}$ is proportional to T_f.

Now, we are concerned with Case (3). Assume that either $u_n := (u_{1n}, u_{2n}) \to u = (u_1, u_2)$ in $(L^1(Q))^2$ or there exists a subsequence, $u^2_n \to u^2$ a.e. on Q. Using Lebesgue's dominated convergence theorem, it comes $\lim_{n\to\infty} \| u^2_n\|_{L^1(Q)} = \|u^2\|_{L^1(Q)}$. The similar arguments is true for $\| v^2\|_{L^1(Q)}$.

Then, we address the convergence of one term in the functional,

$$\| B_1 d(a)(I^{u_n} - I^u) + B_2\psi(a)(S^{u_n} - S^u)\|_{L^1(Q)} \le \max\{B_1\overline{d}, B_2\overline{\psi}\} \| x^{u_n} - x^u\|_{L^1(\mathscr{X})} \le C^1_f \| u_n - u\|_{L^1(Q)}. \tag{3.13}$$

Hence,

$$\| \mathscr{J}(u_n) - \mathscr{J}(u) \| \le C^1_{\mathscr{J}} \| u_n - u\|_{L^1(Q)}.$$

Moreover, we have that $\mathscr{J}(u) \le \liminf_{n\to\infty} \mathscr{J}(u_n)$.

We notice that $\mathscr{J}(u)$ is lower semi-continuous with respect to strong L^1 convergence. However, it is not associated with weak L^1 convergence. Therefore, it generally does not attain its infimum on $\mathscr{U}$. To overcome this default, Ekerland variational principle will be employed to handles this situation (Ekeland, 1974). For $\epsilon > 0$, there exists u_ϵ in $L^1(\mathscr{U})$ such that

$$\begin{cases} \mathscr{J}(u_\epsilon) \le \inf_{u\in\mathscr{U}} \mathscr{J}(u) + \epsilon, \\ \mathscr{J}(u_\epsilon) = \min_{u\in\mathscr{U}} \mathscr{J}(u) + \sqrt{\epsilon}\, \| u_\epsilon - u\|_{L^1(\mathscr{U})}. \end{cases} \tag{3.14}$$

Note that, by the second expression of (3.14), the perturbed functional

$$\mathscr{J}_\epsilon(u) = \mathscr{J}(u) + \sqrt{\epsilon}\, \| u_\epsilon - u\|_{L^1(\mathscr{U})}$$

attains its infimum at u_ϵ. By the same argument as in subsection 3.2 and using the projection map $\mathscr{L}$ on $\mathscr{U}$, we detect a pair of optimal control $(\hat{u}_1, \hat{u}_2)$ such that u_ε minimizes $\mathscr{L}$.

Lemma 2. *If u_ϵ is an optimal control minimizing the functional $\mathscr{J}_\epsilon(u)$,then*

$$u_\epsilon = \mathscr{L}\left(\hat{u}_1(x^{u_\epsilon}, \lambda^{u_\epsilon}) + \frac{\sqrt{\epsilon}\,\pi^\epsilon_1}{A_1}, \hat{u}_2(x^{u_\epsilon}, \lambda^{u_\epsilon}) + \frac{\sqrt{\epsilon}\,\pi^\epsilon_2}{A_2}\right),$$

where $\pi^\epsilon_1, \pi^\epsilon_2 \in L^\infty(Q)$, and $|\pi^\epsilon_i(\cdot,\cdot)| \le 1 (i = 1,2)$, and

$$\hat{u}_1(x^{u_\epsilon}, \lambda^{u_\epsilon}) = \frac{\left((\lambda^{u_\epsilon}_E(t,a) - \lambda^{u_\epsilon}_S(t,a))S^{u_\epsilon} + (\lambda^{u_\epsilon}_E(t,a) - \lambda^{u_\epsilon}_V(t,a))\delta V^{u_\epsilon}(t,a)\right)\int_0^\omega \beta(a,b)\frac{I^{u_\epsilon}}{N^{u_\epsilon}}db}{A_1},$$

$$\hat{u}_2(x^{u_\epsilon}, \lambda^{u_\epsilon}) = \frac{\psi(a)(\lambda^{u_\epsilon}_S(t,a) - \lambda^{u_\epsilon}_V(t,a))S^{u_\epsilon}}{A_2}.$$

Theorem 3.1. *There exists control u^*_1, u^*_2,such that*

$$J(u^*_1, u^*_2) = \min_{\mathscr{U}} J(u_1, u_2).$$

Combining results of Lemma 2 and Theorem 3.1, the following Theorem gives a sufficient condition of the existence of a unique optimal control.

Theorem 3.2. *If* $C_{\mathscr{G}}\left(\frac{1}{A_1}+\frac{1}{A_2}\right)$ *is sufficiently small, there exists a unique optimal control* u* *in* $\mathscr{U}$ *minimizing* $\mathscr{J}(u)$.

Proof. Define $\mathscr{G}:\mathscr{U}\to\mathscr{U}$ by

$$\mathscr{G}(u)=\mathscr{L}(\hat{u}_1(x^{u_\epsilon},\lambda^{u_\epsilon}),\hat{u}_2(x^{u_\epsilon},\lambda^{u_\epsilon})),$$

where x^u and λ^u are state and adjoint solutions associated with control u. By using Lipschitz properties of x^u and λ^u, for every $u,v\in\mathscr{U}$, one reaches

$$\begin{aligned}&\|\mathscr{L}_1(u_1)-\mathscr{L}_1(v_1)\|_{L^\infty(\mathscr{X})}\\ &=\left\|\frac{(\lambda_E^u-\lambda_S^u)S^u(t,a)\int_0^\omega\beta(a,b)\frac{I^u(t,b)}{N^u(t,b)}db}{A_1}-\frac{(\lambda_E^v-\lambda_S^v)S^v(t,a)\int_0^\omega\beta(a,b)\frac{I^v(t,b)}{N^v(t,b)}db}{A_1}\right\|_{L^\infty(\mathscr{X})}\\ &\le\frac{C_{\mathscr{L}_1}}{A_1}\|u-v\|_{L^\infty(\mathscr{U})}\end{aligned}$$

In the same way, we also have

$$\|\mathscr{L}_1(u_2)-\mathscr{L}_1(v_2)\|_{L^\infty(\mathscr{X})}\le\frac{C_{\mathscr{L}_2}}{A_2}\|u-v\|_{L^\infty(\mathscr{U})}.$$

Consequently,

$$\|\mathscr{G}(u)-\mathscr{G}(v)\|_{L^\infty(\mathscr{X})}\le C_{\mathscr{G}}\left(\frac{1}{A_1}+\frac{1}{A_2}\right)\|u-v\|_{L^\infty(\mathscr{U})},\tag{3.15}$$

where the constant $C_{\mathscr{L}}$ depends on the L^∞ bounds on the state and adjoint solutions, and Lipschitz constants. The functional $\mathscr{G}$ has a unique fixed point u* when $C_{\mathscr{L}}\left(\frac{1}{A_1}+\frac{1}{A_2}\right).<1$.

Then, the key is to prove that the fixed point is an optimal control. By using the approximate minimizers u_ϵ by Ekerland variational principle, and combining Lemma 2 with the scaling of $\mathscr{G}$, we find that

$$\begin{aligned}\|\mathscr{G}(u_\epsilon)-u_\epsilon\|_{L^\infty(\mathscr{X})}&=\|\mathscr{L}(\overline{u}_1(x^{u_\epsilon},\lambda^{u_\epsilon}),\overline{u}_2(x^{u_\epsilon},\lambda^{u_\epsilon}))-\mathscr{L}\left(\overline{u}_1(x^{u_\epsilon},\lambda^{u_\epsilon})+\frac{\sqrt{\epsilon}\,\pi_1^\epsilon}{A_1},\overline{u}_2(x^{u_\epsilon},\lambda^{u_\epsilon})+\frac{\sqrt{\epsilon}\,\pi_2^\epsilon}{A_2}\right)\|_{L^\infty(\mathscr{X})}\\ &\le\|\frac{\sqrt{\epsilon}\,\pi_1^\epsilon}{A_1}\|_{L^\infty(Q)}+\|\frac{\sqrt{\epsilon}\,\pi_2^\epsilon}{A_2}\|_{L^\infty(Q)}\\ &\le\sqrt{\epsilon}\left(\frac{1}{A_1}+\frac{1}{A_2}\right).\end{aligned}\tag{3.16}$$

With the help of inequalities (3.15) and (3.16), we have

$$\begin{aligned}&\|u^*-u_\epsilon\|_{L^\infty(\mathscr{U})}=\|\mathscr{G}(u^*)-u_\epsilon\|_{L^\infty(\mathscr{X})}\\ &\le\|\mathscr{G}(u^*)-\mathscr{G}(u_\epsilon)\|_{L^\infty(\mathscr{X})}+\|\mathscr{G}(u_\epsilon)-u_\epsilon\|_{L^\infty(\mathscr{X})}\\ &\le C_{\mathscr{G}}\left(\frac{1}{A_1}+\frac{1}{A_2}\right)\|u^*-u_\epsilon\|_{L^\infty(\mathscr{U})}+\sqrt{\epsilon}\left(\frac{1}{A_1}+\frac{1}{A_2}\right).\end{aligned}$$

Since $C_{\mathscr{G}}$ is proportional to T_f, $\frac{T_f}{2}\left(\frac{1}{A_1}+\frac{1}{A_2}\right)$ is sufficiently small. Hence, it comes that

$$\|u^*-u_\epsilon\|_{L^\infty(\mathscr{U})}\le\frac{\sqrt{\epsilon}\left(\frac{1}{A_1}+\frac{1}{A_2}\right)}{1-C_{\mathscr{G}}\left(\frac{1}{A_1}+\frac{1}{A_2}\right)}.$$

Thus, an approximate minimiter u_ϵ converges to the fixed point u*, namely $u_\epsilon\to u^*$ in $L^\infty(\mathscr{U})$, and by using Ekelands's principle (as $\epsilon\to 0$)

$$\mathscr{J}(u^*)\le\inf_{u\in\mathscr{U}}\mathscr{J}(u).$$

4. Numerical simulations

To visibly observe the control effects, we are conducted to numerical experiments to capture them. To achieve this goal, we employ the forward-backward sweep approach (Lenhart & Workman, 2007). Actually, a forward fourth-order Runge-Kutta method is done for the state variables and a backward fourth-order Runge-Kutta method is designed for the adjoint variables (Martcheva, 2015b).

For suppressing an emerging infectious disease, we introduce two elementary controls: physical distancing u_1 and vaccination u_2. To take account effects for every feasible control, we classify the following four strategies:

- Strategy A measures to reduce physical distancing;
- Strategy B measures to increase vaccination rate;
- Strategy C measures to take coupled controls;
- Strategy D measures no control strategy(blank group).

4.1. Parameter selection

In order to ensure the authenticity and validity of the investigation, we select data from the initial COVID-19 outbreak in Sao Paulo, Brazil for numerical simulation. According to the transmission characteristics of COVID-19 infection in Brazil, the total population is divided into six age groups: 0–9 years old, 10–39 years old, 40–49 years old, 50–59 years old, 60–69 years old and over 70 years old. The transmission rate $\beta(a, b)$ is taken in form of

$$\beta(a,b) = \beta \times c(a,b), \tag{4.1}$$

where β denotes the effective transmission probability and $c(a, b)$ represents the number of physical contacts per day between susceptibles with age a and infectives with age b. For the convenience, we define the contacts during each group are constants and so it generates a contact matrix (see Fig. 1).

Other parameters used in the simulation are taken in Table 1, as well as the initial values of state variables for each age group are selected from Table 2 (Rocha Filho et al., 2020).

- Step one

To evaluate the control effects, judiciously controlling cost of the strategy is an important index, which needs to mitigate financial burden without jeopardizing the most vulnerable members of the population (Zhao & Feng, 2020). Since the major purpose of optimal control questions is to balance revenue and costs of the controls, we take three typical cases to reflect their effects: (1) low cost, that is, $A_1 = A_2 = 1$; (2) moderate cost, that is, $A_1 = A_2 = 100$; (3) high cost, that is, $A_1 = A_2 = 1000$. Now we are going to investigate the total number of infected persons in six age groups.

Fig. 2 shows the total number of infected cases under strategy $A - D$. It is clear that each control strategy reduces the size of the prevalence, shortens the epidemic duration, advances the peak arrived time and deduces the peak values. Conversely, the decreasing trends rank: low-cost control, median-cost control, high-cost control. Therefore, the control cost is the key to disease prevention and control.

Next, we will analyze the question in a quantitative perspective, that is focusing on the values of the objective function at different costs under different strategies (see Table 3). A clear observation is that under the same strategy, the more the cost is, the bigger the corresponding to objective function value will be, which means that the higher the control cost is, the worse the control effect will be. Under the same cost, the objective function value correspondingly strategy C is smaller than that of other strategies, that is, strategy C is optimal with the least cost. We further analyze the specific effects of strategy C for different age groups. As observed in Fig. 3, compared with no control, infection peaks in all age groups decrease and the peak arrived times reach earlier after the implementation of strategy C. The prevalence decreases the fastest for the group aged 10–39 and reduces the lowest for the group over 70 years old.

In the comparative analysis, we find that the difference between strategy A and strategy C is subtle. To further distinguish the effects of the implementation of two strategies, we are conducted to quantitative evaluation, which could be globally analyzed from three aspects: the total number of infected cases in $0 - T$ period, the number of persons who avoids becoming infected as a result of the implementation of the control in the $0 - T$ period and objective function value. According to Table 5, compared with other strategies, strategy C (i.e. the combination strategy) had the lowest number of infections within $0 - T$, and more people avoided becoming infected. At the same time, the objective function value of strategy C is the smallest, which indicates that strategy C can save manpower and material resources and prevent more susceptible individuals from becoming infected persons. Therefore, the mixed measure simultaneously increasing social distancing and vaccination is a dominant strategy.

In order to quantify the effects of strategy C on each age group, we define an Infection Averted Rate(IAR) (Okosun et al., 2013) by

$$IAR = \frac{Number\ of\ people\ who\ avoid\ infection}{Infectious\ individuals\ without\ control},$$

where the number of persons who avoided infection is the number of infected persons caused without control minus the number of infected persons with control. Table 4 shows that the rank of the IAR values are people aged 60–69, aged over 70, aged 10–39, aged 0–9, aged 40–49 and aged 50–59. Clearly, strategy C takes better significant effects on people aged 10–39 and over 60 (see Table 4).

- Step two

From (Arnold et al., 2021), we have known that vaccination is a highly cost-effective action than that taking social distancing measures for control COVID-19. Then, we set weight coefficients $A_1 = 1$, $A_2 = 1000$, $A_3 = 1$, $B = 1$, evaluate effects of feasible control measures and then look for an optimal control measure associated with each age group.

Fig. 4 displays that the implementation of strategy A, B and C deduces peaks values and advance the peak arrived time. Further analysis shows that compared with other strategies, enlarging physical distancing enables the prevalence peak arrives faster, and the slope of decline after the peak is sharper, which suggests that physical distancing measure, such as limiting gathering, closing building, working at home, etc., plays a significant role in preventing the infections. For each strategy, the prevalence are lowest for people aged over 60, which indicates that the control effects are beneficial for people aged over 60.

Table 6 and Fig. 5 give the durations of strong control measures and the optimal controls associated each age group. Under the optimal control strategy C, the durations of strongly increasing social distancing and strengthening vaccination for aged 10–39 need 27.24 and 57.18 days, respectively. Conversely, such durations are obviously longer than the durations of other age groups. On the other hand, the duration of intensive vaccination control is almost double than that duration of increasing social distancing in the same age group. This finding has an important implication for the actual allocation of medical resources for the disease prevention and control. In this case, the policymakers and the public health governments should pay more attention on controlling payoffs in the group aged 10–39. Especially, they should markedly note that the effective control impacts of taking vaccination should be a longer patience.

5. Discussion

Age heterogeneity is a noteworthy features of many emerging infectious diseases, which has well-known impact on the magnitudes and intensity of such diseases. In this paper, we introduced a continuous age-structured model to study the transmission dynamics of emerging infectious diseases in a short period or in the initial outbreak. Since some emerging infectious diseases are highly sensitive due to a higher social activity in certain age groups. We tried to identify the age groups to target for effectively slowing down the disease infection.

In this paper, we calculated the basic reproduction number $\mathscr{R}_0$, which is a spectral radius of the next generation operator $\mathscr{K}$. The value of $\mathscr{R}_0$ determines the stability of the disease-free equilibrium E_0. If it is less than 1, then E_0 is globally asymptotically stable by constructing a suitable Lyapunov function. In such construction, we employed the left eigenvector of $\mathscr{K}$ as a kernel function to completely address the global stability of E_0, which provides a new approach for dealing with the global stability of continuous age-structured models.

Facing a novel emerging diseases, maintaining social distance and projecting vaccination are two main control measures for curtaining the diseases infection. However, because of the economic and social burdens and limitations of medical resources, identifying optimal control measures has become an urgent issue. In this paper, we tried to evaluate the two control strategies and found the optimal control strategies by cost-effective analysis. Moreover, we derived the adjoint system and optimal control pairs by constructing a generalized Hamilton functional. As the continuous age-structured model is characterized by a series of first order partial differential equations, the optimal problems are quietly different from the problems describing by a second order PDE system, due to the lack of the regularity of the state solutions. To overcome this default, we employed Ekeland Principle's to analyze the existence of the optimal control, such methods have been extensively used by many scholars (Barbu, 1994; Barbu & Iannelli, 1999; Numfor et al., 2014; Yang et al., 2019). We pointed out that if the weight parameters are sufficiently large or the control target time T is small enough, such optimal control exists from mathematical view of points.

In order to illustrate our theoretical results, we picked up an initial outbreak of COVID-19 in Sao Paulo, Brazil. We proposed three different control measures such as single reducing physical distance, single vaccination and mixed the two measures to take account for the impact on the control COVID-19. We found that reducing physical distance is necessary for the initial outbreak of COVID-19 and vaccination is most effective for a long-term outbreak. Conversely, the effect of the mixed strategy is more significant under the low cost and this control strategy is most effective for old peoples and the young age group. Overall, the combination of enlarging social distance and the mass vaccination is the most cost-effective. Meanwhile, the primary target of the two control variables is the group aged 10–39, which means that the Brazil government should take more investments on people aged 10–39 for the prevention and control COVID-19 infection.

For the age-structured models, model parameters are generally assumed to change with the activity of people in different ages such as death rate due to diseases, latent period, recovered period etc. As it reported, environment-to-human has

become a non-negligible transmission route of COVID-19. Furthermore, pathogenic mutation, human behaviors and other factors have great effects on the transmission of emerging infectious diseases, we will leave these work for the future.

Declaration of competing interest

The authors declare that they have no known competing financial interests or personal relationships that could have appeared to influence the work reported in this paper.

Acknowledgement

The authors are very grateful to the associated editor and the anonymous referees for their valuable comments and suggestions, which helped us to improve the presentation of this work significantly.

This work was partially supported by the National Natural Science Foundation of China (NNSFC) (Nos. 12 001 339, 61 573 016, and 11 771 017), the Shanxi Province Science foundation (20210302123454), the Shanxi Province Science Foundation for Youths (No.201901D211413), and the Shanxi Scholarship Council of China (No. 2015-094).

References

Agua-Agum, J., Ariyarajah, A., Aylward, B., & Bawo, L. (2016). Exposure patterns driving ebola transmission in west africa: A retrospective observational study. *PLoS Medicine, 13*(11), Article e1002170.

Ahmed, R., Williamson, M., Hamid, M. A., & Ashraf, N. (2020). United States county-level covid-19 death rates and case fatality rates vary by region and urban status. *Healthcare (Basel), 8*(3), 330.

Anderson, R. M., & May, R. M. (1974). Age-related changes in the rate of disease transmission: Implications for the design of vaccination programmes. *Journal of Hygiene, 94*, 365–436.

Arnold, H., İnkaya, A.Ç., Yildirak, K., Sancar, M., van der Schans, J., Sancar, A. A., Ünal, S., Postma, M., & Yeğenoğlu, S. (2021). Covid-19 vaccination scenarios: A cost-effectiveness analysis for Turkey. *Vaccines, 9*(4), 399.

Barbu, V. (1994). *Mathematical methods in optimization of differential systems*. Kluwer Academic Publishers.

Barbu, V., & Iannelli, M. (1999). Optimal control of population dynamics. *Journal of Optimization Theory and Applications, 102*, 1–14.

Beutels, P. (1988). Economic evaluations applied to hb vaccination:general observation. *Vaccine, 16Suppl*, 84–92.

Blayneh, K., Cao, Y., & Kwon, H.-D. (2009). Optimal control of vector-borne diseases: Treatment and prevention. *Discrete & Continuous Dynamical Systems-B, 11*(3), 587.

Cauchemez, S., Nouvellet, P., Cori, A., et al. (2016). Unraveling the drivers of mers-cov transmission. *Proceedings of the National Academy of Sciences of the United States of America, 113*(32), 9081–9086.

Demasse, R. D., Tewa, J.-J., Bowong, S., & Emvudu, Y. (2016). Optimal control for an age-structured model for the transmission of hepatitis b. *Journal of Mathematical Biology, 73*(2), 305–333.

Ekeland, I. (1974). On the variational principle. *Journal of Mathematical Analysis and Applications, 47*, 324–353.

Epidemiology Team. (2020). The epidemiological characteristics of an outbreak of 2019 novel coronavirus diseases (covid-19)?China. *China CDC Weekly, 2*(8), 113, 2020.

Eslami, H., & Jalili, M. (2020). The role of environmental factors to transmission of sars-cov-2 (covid-19). *AMB Express, 10*(1), 92.

Fraser, C., Donnelly, C. A., Cauchemez, S., et al. (2009). Pandemic potential of a strain of influenza a (h1n1): Early findings. *Science, 324*(5934), 1557–1561.

Gao, P., Xu, G., Chen X Li, C., & Wang, Z. (2016). Age-period-cohort analysis of infectious disease mortality in urban-rural China,1990-2010. *International Journal for Equity in Health, 15*(55).

Ghani, A. C., Donnelly, C. A., Cox, D. R., et al. (2005). Methods for estimating the case fatality ratio for a novel, emerging infectious disease. *American Journal of Epidemiology, 162*, 479–486.

Glass, L. M., abd Glass, R. J., Beyeler, W. E., et al. (2006). Targeted social distancing design for pandemic influenza. *Emerging Infectious Diseases, 12*(11), 1671–1681.

Gojovic, M. Z., Sander, B., & Fisman, D. (2009). Modelling mitigation strategies for pandemic (h1n1) 2009. *Canadian Medical Association Journal, 181*, 673–680.

Jones, K. E., Patel, N. G., Levy, M. A., et al. (2008). Global trends in emerging infectious diseases. *Nature, 451*, 990–993.

Kwon, H.-D., Lee, J., & Yang, S.-D. (2012). Optimal control of an age-structured model of hiv infection. *Applied Mathematics and Computation, 219*(5), 2766–2779.

Lazarus, J. V., Ratzan, S. C., Palayew, A., Gostin, L. O., Larson, H. J., Rabin, K., … Ei-Mohandes, A. (2021). A global survey of potential acceptance of a COVID-19 vaccine. *Nature Medicine, 27*(2), 225–228.

Lee, S., Golinski, M., & Chowell, G. (2012). Modeling optimal age-specific vaccination strategies against pandemic influenza. *Bulletin of Mathematical Biology, 74*(4), 958–980.

Lenhart, S., & Workman, J. T. (2007). *Optimal control applied to biological models*. Chapman and Hall/CRC.

Lev Semenovich Pontryagin. (1987). *Mathematical theory of optimal processes*. CRC press.

Linton, N. M., Kobayashi, T., Yang, Y., Hayashi, K., Akhmetzhanov, A. R., Jung, S.-mok, Yuan, B., Kinoshita, R., & Nishiura, H. (2020). Incubation period and other epidemiological characteristics of 2019 novel coronavirus infections with right truncation: A statistical analysis of publicly available case data. *Journal of Clinical Medicine, 9*(2), 538.

Li, X. Z., Yang, J. Y., & Martcheva, M. (2020). *Age structured epidemic modelling*. Springer.

Majumder, M. S., Hess, R., Ross, H., & Piontkivska, R. (2018). Seasonality of birth defects in west africa: Could congenital zika syndrome be to blame? *F1000Research, 7*, 159.

Martcheva, M. (2015a). *An introduction to mathematical epidemiology*. Springer.

Martcheva, M. (2015b). *An introduction to mathematical epidemiology* (Vol. 61). Springer.

Matrajt, L., Eaton, J., Leung, T., & Brown, E. R. (2021). Vaccine optimization for covid-19: Who to vaccinate first? *Science Advances, 7*(6), Article eabf1374.

Metz, J. (1978). The epidemic in a closed population with all susceptibles equally vulnerable; some results for large susceptible populations and small initial infections. *Acta Biotheoretica, 27*(1–2), 75–123.

Numfor, E., Bhattacharya, S., Lenhart, S., & Martcheva, M. (2014). Optimal control applied in coupled within-host and between-host models. *Mathematical Modelling of Natural Phenomena, 9*, 171–203.

Oei, H., & Nishiura, W. (2012). The relationship between tuberculosis and influenza death during the influenza (h1n1) pandemic from 1918-19. *Comput. Math. Methods Med.*, 124861, 2012.

Okosun, K. O., Rachid, O., & Marcus, N. (2013). Optimal control strategies and cost-effectiveness analysis of a malaria model. *Biosystems, 111*(2), 83–101.

Rocha Filho, T. M., dos Santos, F. S. G., Gomes, V. B., Rocha, T. A. H., Croda, J. H. R., Ramalho, W. M., & Araujo, W. N. (2020). *Expected impact of covid-19 outbreak in a major metropolitan area in Brazil*. medRxiv.
Wang, C., Horby, P. W., Hayden, F. G., & Gao, G. F. (2020). A novel coronavirus outbreak of global health concern. *Lancet, 395*(10223), 470–473.
Wendell, H. F., & Rishel, R. W. (2012). *Deterministic and stochastic optimal control* (Vol. 1). Springer Science & Business Media.
Yang, J. Y., Modnak, C., & Wang, J. (2019). Dynamical analysis and optimal control simulation for an age-structured cholera transmission model. *Journal of the Franklin Institute, 356*, 8438–8467.
Zhao, H., & Feng, Z. (2020). Staggered release policies for covid-19 control: Costs and benefits of relaxing restrictions by age and risk. *Mathematical Biosciences, 326*, 108405.